Experimental Outlook for Virtual Compton Scattering at High Energy

Charles Hyde-Wright*, Pierre-Yves Bertin†
*Old Dominion University, Norfolk VA 23529 USA
†LPC, Université Blaise Pascal 63177 Aubière FRANCE

I. INTRODUCTION

The real and virtual compton scattering reactions $\gamma + p \to \gamma + p$ and $e + p \to e + p + \gamma$ at 6-12 GeV provide many important new areas of study of QCD and proton structure. There are new theoretical results suggesting that for either large $P'_\perp$ (s, t, u all large) **or** large Q^2, the compton process can be described by the handbag diagram of Fig. 1. [1–4] The amplitude of Fig. 1 is the convolution of the elementary $\gamma q \to \gamma q$ kernel with a new class of ground state matrix elements, called the off-forward parton-distributions (OFPD). This description should be contrasted with the asymptotic prediction (probably valid only at much higher energies) also shown in Fig. 1. In the latter case, the compton amplitude is given by a hard scattering kernel consisting of all possible gluon exchange diagrams convoluted with the product of the initial and final state distribution amplitudes. [5–8] The experimental VCS process also includes an important contribution from the Bethe-Heitler (BH) terms (wide angle bremsstrahlung). The BH-Compton interference terms are experimentally accessible via the following observables (ϕ is the azimuthal angle of the proton around the VCS virtual photon direction): a) the $\cos\phi d\sigma_{LT}$ term; b) the electron helicity asymmetry $d\Sigma = d\sigma(\overrightarrow{e}, e'p) - d\sigma(\overleftarrow{e}, e'p)$ (measured out-of-plane); and c) the electron-positron difference cross section $d\sigma(e^+, e^{+\prime}p) - d\sigma(e^-, e^{-\prime}p)$. In a) & b), the specific sensitivity to the BH term results when the longitudinal part of the compton amplitude is much smaller than the corresponding BH term.

In Sec. III we discuss the specific issues associated with **Hard Scattering**: $s = (q + P)^2$ large, $P'_\perp$ large, $(0 \ll \theta_{\gamma,\gamma} \ll \pi)$, and arbitrary Q^2. In Sec. IV we discuss **Deeply Virtual Compton Scattering** (DVCS): s, & Q^2 large, $\theta_{\gamma,\gamma} \approx 0$, $t = (q - q')^2 \approx -M^2 x_{\rm Bj}^2/(1 - x_{\rm Bj})$.

II. OFF FORWARD PARTON DISTRIBUTIONS

The off forward parton distributions are defined as the amplitude to remove a parton from the proton at point $y/2$ on the light cone and replace it in the final state proton at point $-y/2$. The OFPD are functions of the momentum fraction x (the fourier transform variable conjugate to the

coordinate y), the kinematic variable $\xi/2 \approx Q^2/q \cdot (P + P') \approx x_{\rm Bj}$ and the invariant momentum transfer $t = (q - q')^2$. Neglecting QCD evolution, the OFPD are Q^2 independent. On the proton, there are four OFPD corresponding to helicity conserving and helicity flip matrix elements of the vector and axial-vector operators $\overline{\psi}\gamma_\alpha\psi$ and $\overline{\psi}\gamma_\alpha\gamma_5\psi$. In the $(\xi, t) \to (0, 0)$ limit the helicity conserving vector and axial-vector OFPD are equal to the ordinary parton distributions $q(x)$ and $\Delta q(x)$, respectively. At fixed $t = (P' - P)^2$, the integral over x of the OFPD are equal to the corresponding elastic form-factors $F_{1,2}(-t)$, $G_{A,P}(-t)$. The compton process weights the flavor dependent OFPD with the quark charge squared whereas the elastic (e, e') form factors are weighted by one power of the quark charge. Thus compton scattering provides new information for the flavor decomposition of the proton. The helicity flip OFPD are linked to quark orbital angular momentum distributions. This is elegently illustrated by the sum-rule of X. Ji [1] which directly links the vector OFPD to the orbital angular momentum contribution to the quark spin.

III. HARD SCATTERING

Real and virtual compton scattering in the hard scattering domain at 6 GeV are the subjects of Exp.97-108 [9,10] and Exp.94-106. [11] The handbag dominance of this reaction has been discussed by A. Radyushkin. [4] In high energy VCS, it is necessary to detect all three final state particles in order to separate inelastic channels and accidental backgrounds. Recent measurements in Hall-A suggest that the very low emittance CEBAF beam will permit the use of a unshielded Pb-glass array at luminosity $\mathcal{L} = 2 \cdot 10^{38}/\mathrm{cm}^2/\mathrm{s}$ for $\theta_\gamma > 30^\circ$. In the wide angle compton case, if a septum magnet can be used to detect electrons at 6°, then count rates of ≥ 10/hour can be achieved in the Hall-A HRS^2 pair for $s \leq 10$ GeV^2, $90 \leq \theta_{\gamma\gamma}^{\rm CM} \leq 120^\circ$, and $Q^2 \leq 0.5$ GeV^2.

The Q^2 dependence of high $P_\perp$ VCS measurements at low Q^2 and the magnitude of the imaginary part of the compton amplitude (accessible in VCS via the electron helicity dependent cross section $d\Sigma$) are important tools for identifying the basic reaction process in this energy regime. If the HandBag amplitude dominates the compton amplitude, then the imaginary part of the hard scattering compton amplitude is small.On the other hand, in the hard-gluon exchange pQCD amplitude the imaginary part of the the compton amplitude is large. This is a general feature of any model incorporating hard exchanges (see for example the di-quark model [8,12]).

Small angle θ_e electron scattering (for small Q^2) naturally gives a large out-of-plane acceptance for the measurement of $d\Sigma$. With the electron spectrometer at 6°, the azimuthal acceptance of the HRS pair is $\sin\phi = \pm\tan\theta_V / \sin\theta \approx \pm 0.5$.

In the handbag amplitude for VCS, the Q^2 dependence is dominated by the elementary $\gamma^* + q \to \gamma + q$ amplitude (the ξ dependence of the OFPD is weak [13]). This is not the case, for example, in the di-quark model. [13] Thus VCS measurements, even at low Q^2 are an important test of the handbag dominance hypothesis.

IV. DVCS

The experimental challenges of DVCS include: a) Small cross sections: for electron energies from 6 to 11 GeV and $Q^2 = 2$ - 4 GeV^2 the cross section $d^5\sigma/[d\Omega_e E'_e d\Omega_{\gamma\gamma}] \approx 100\text{pb}/[\text{sr}^2\text{GeV}]$ at $x_{\rm Bj} \approx 0.3$; b) The BH cross section is typically 10× the DVCS cross section; c) The electron and photon are both at small angles ($\approx 10°$) from the beam direction; d) The recoil protons are emitted at small momentum: at $\theta_{\gamma\gamma} = 0$, $p'_p \approx M x_{\rm Bj}[1-x_{\rm Bj}/2]/[1-x_{\rm Bj}]$; e) It is difficult to separate the exclusive $ep \to e\gamma p$ channel from competing background channels, e.g. $ep \to e\pi^0$ and $ep \to e\gamma N^*$.

At CEBAF energies, the BH amplitude must be used as an amplifier and a filter. For energies $6 - 12$ GeV, a kinematic range $2 < Q^2 < 4$ GeV^2 and $x_{\rm Bj} > 0.3$ is accessible, though the OFPD decrease rapidly for large $x_{\rm Bj}$. For photon emission angles relative to the virtual photon direction as small as 5°, the electron helicity asymmetry A_h is as large as 30%. In both the helicity dependent and helicity independent cross sections the Q^2 dependence of each $\cos n\phi$ and $\sin n\phi$ term is directly predicted by the HandBag dominance hypothesis, independent of the models of the OFPD. [14] Thus measurements of the full ϕ dependence around the virtual photon direction are an essential test of the DVCS formalism. Fig. 2 illustrates the statistical precision and azimuthal acceptance feasible in Hall-A with the electron spectrometer in coincidence with a 10 msr photon calorimeter. Similar results can be obtained at energies of 9 and 11 GeV and $Q^2 = 3$, 4 GeV^2.

The electron-positron cross section difference is also an attractive possibility for extracting the DVCS amplitude. Electrons and positrons can be accelerated in tandem in the North Linac, with the two beams 180° out of phase in the RF. At the arcs, the positron beam is recirculated for the desired number of turns, and the electron beam is diverted to a positron

production target. The positrons can be brought back to the injection area via a beam line inside the main tunnel. A beam of +10 nA will be adequate to simultaneously provide a positron luminosity of $10^{34}/\mathrm{cm}^2/\mathrm{sec}$ in Hall-B and the full photon luminosity in Hall-D.

At 6 GeV, a photon calorimeter with resolution $5\%\sqrt{GeV/q'}$ is sufficient to separate the $p(e,e'\gamma)p$ peak from the $p(e,e'\gamma)N\pi$ threshold by 3σ. However, at higher energies this separation requires an overcomplete determination of the final state. In the kinematics of CEBAF below 12 GeV, this means detecting the recoil protons in a cone around the virtual photon direction $10^\circ < \theta_p < 40^\circ$ and 300 MeV $< p' <$ 800 MeV (the momentum and angle are correlated). It is not necessary to identify the proton or measure its absolute momentum. For a given $p(e,e'\gamma)X$ event, detecting a charged particle in the direction required for an exclusive $p(e,e'\gamma p)$ event will be adequate to remove the background channels (except possibly the $ep \to e\gamma p\pi^0$ exactly at $p\pi^0$ threshold. The high rate detectors (Multi Strip Gas Detectors, etc.) discussed in this workshop (Ref. [15,16]) offer the possibility of detecting the recoil protons. A 1-2 Tesla axial field is required at the target to trap particles with $P_\perp < 20$ MeV. The natural pixel size for a recoil detector is $\Delta\theta \otimes \Delta\phi = (100mr) \otimes (10mr)$, corresponding to the reconstruction resolution from the $p(e,e'\gamma)X$ measurement. At a distance of 0.5 m from the target, the load of random charged particles with be less than 10^5 per pixel. [17] Detecting the recoil particle also offers the prospect of measuring deuteron OFPD via $D(e,e'\gamma D)$.

It should also be noted that the"background" channels discussed above are of interest in their own right. The "Deep π" process $ep \to ep\pi^0$ is described by the convolution of a one gluon exchange kernel, the pion distribution amplitude, and the same axial OFPD as in the DVCS case. [18] The inclusive DVCS process $ep \to e\gamma N^*$ is sensitive to the inelastic $p \to N^*$ OFPD. [19]

V. SPECTROMETERS VS. LARGE ACCEPTANCE

A priori, the exclusive $ep \to ep\gamma$ reaction requires high resolution, thus favoring the Hall-A HRS^2 pair. However, with sufficient hermeticity, the overcompleteness of the reaction can be used to identify the exclusive channel in a large acceptance detector such as the CLAS.

In Deeply virtual compton scattering, the photon is highly correlated with the electron, so we assume the Hall-A acceptance is limited by the electron arm. At $E_e = 11$ GeV, $Q^2 = 4$ GeV, and $x_{\mathrm{Bj}} = 0.3$ the in-

plane acceptance of the electron arm is $\Delta Q^2 \Delta x_{\rm Bj} = 0.033$ GeV^2 and the out-of-plane acceptance is $\Delta\phi = \sin^{-1}[\tan\theta_V / \sin\theta_e] = 400$ mr. We also assume a Hall-A luminosity of $10^{37}/\mathrm{cm}^2/\mathrm{s}$ limited by a combination of the photon calorimeter and the detectors required to tag the direction of the outgoing proton. In the CLAS we can take a natural bin size of $\Delta Q^2 \Delta x_{\rm Bj} = (1.0 GeV^2) \cdot (0.1)$, an azimuthal acceptance of 1.5π and $\mathcal{L} = 10^{34}/\mathrm{cm}^2/\mathrm{s}$. The relative counting rate in the two scenarios is [Hall-A]/[Hall-B] ≈ 30. Of course in Hall-B many bins in Q^2 and $x_{\rm Bj}$ can be obtained simultaneously. In Hall-B, $\mathcal{L} > 10^{34}/\mathrm{cm/s}$ may be possible by requiring that the shower sum in two opposing sectors equal the beam energy (within resolution).

In the Hard Scattering regime,at low Q^2, the HRS electron arm acceptance defines a natural bin size in $Q^2 \otimes s$. To compare the two scenarios, we integrate over the same acceptance in $d\cos\theta_e dE'_e$. In Hall-A we integrate over the electron vertical angle acceptance and the proton HRS acceptance. In Hall-B we integrate over the the full azimuth for both the electron and the proton and we integrate over a bin $\Delta\cos\theta^{\rm CM}_{\gamma\gamma} = 0.2$. We also weight the acceptance by $\sin^2\phi_{\gamma\gamma}$ to compare the figure of merit for measuring $d\Sigma$ in each Hall. At $s = 10$ GeV^2, $Q^2 = 0.5$ GeV^2, $\theta^{\rm CM}_{\gamma\gamma} = 90^\circ$, we obtain a ratio of weighted counting rates per bin $(Q^2, s, \theta^{\rm CM}_{\gamma\gamma})$ of [Hall-A]/[Hall-B] ≈ 40 at $\mathcal{L}_A/\mathcal{L}_B = 2 \cdot 10^{38}/10^{34}$.

VI. CONCLUSIONS

These experiments offer many exciting prospects for studying both the nature of QCD and nucleon structure. The three experimental options: Large Acceptance Spectrometer, Spectrometer pair with photon calorimeter, or Spectrometer with photon calorimeter and recoil detector offer important possibilities for these measurements.

---

[1] X. Ji, Phys.Rev.Lett.78:610-613,1997, & Phys.Rev.D55:7114-7125,1997.
[2] A.V. Radyushkin, Phys Lett **B380** (1996) 417, hep-ph/9604317.
[3] J.C. Collins, A. Freund hep-ph/9801262.
[4] A.Radyushkin, hep-ph/9803316.
[5] S.J. Brodsky and G. Farrar, Phys. Rev. Lett. **31** (1973) 1953.
[6] Glennys R. Farrar and Huayi Zhang, PRL **65**, (1990) 1721, & PR**D41** (1990) 3348, and E. Maina and G.R. Farrar, PL**B206** (1988) 120.
[7] A.S. Kronfeld and B. Nizic, Phys Rev **D44** (1991) 3445.
[8] P.A.M. Guichon & M. Vanderhaeghen, Prog Part Nucl Phys **41** (1998)125.
[9] A. Nathan, these proceedings

[10] J.P. Chen, et al, Jefferson Laboratory Exp 97-108
[11] G. Audit, et al, Jefferson Laboratory Exp.94-106.
[12] P. Kroll, M. Schürmann, and P.A.M. Guichon, Nucl Phys **A598**, 435 (1996).
[13] X. Ji, W. Melnitchouk, and X. Song, Phys Rev **D56**, 5511 (1997).
[14] T.Gousset, et al., hep-ph/9712267, & M.Diehl et al., PL **B411**, 193 (1997).
[15] P. Weilhammer, H. Weiman, these proceedings
[16] F. Sauli, CERN-EP-98-051, Mar 1998, 8th Vienna Wire Chamber Conf.
[17] P. Degtiarenko, code GDINR, private communication 1998.
[18] J.C. Collins et alia, Phys.Rev.D56:2982-3006,1997 hep-ph/9611433
[19] M. Polyakov, these proceedings.

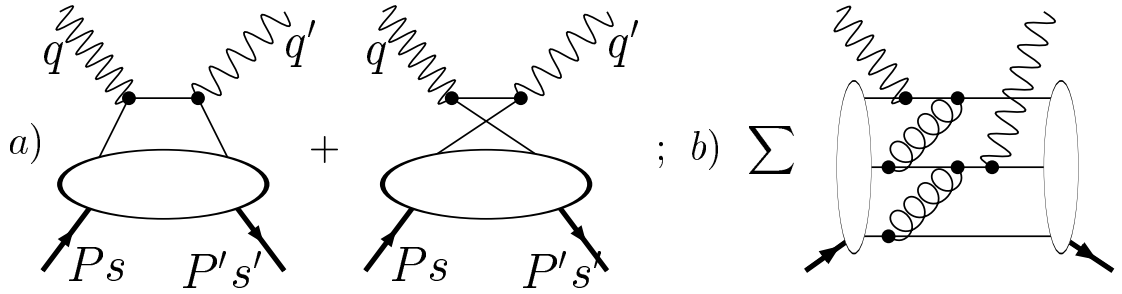

FIG. 1. Two approximations to Real or Virtual Compton scattering amplitude: a) Hand-Bag approximation; b) asymptotic Perturbative QCD .

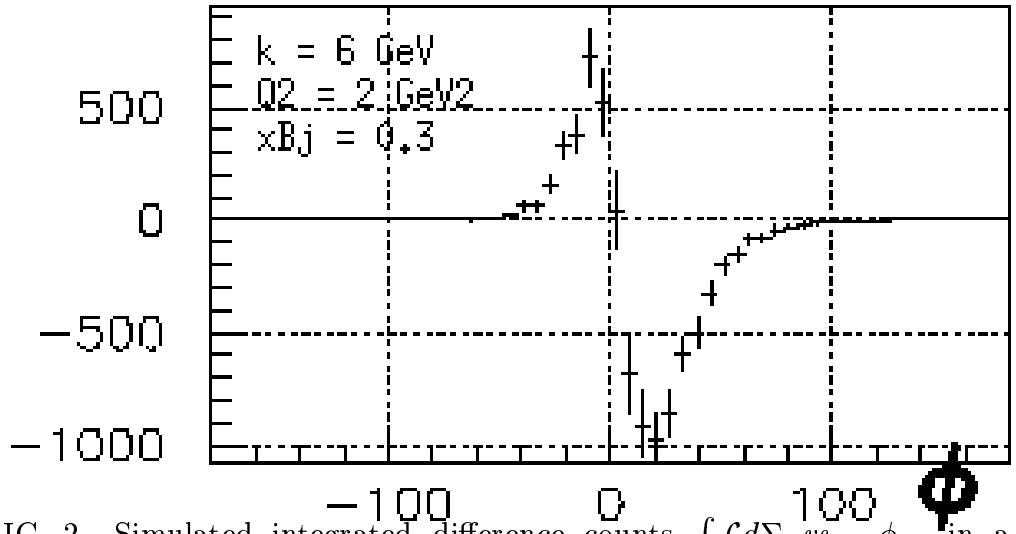

FIG. 2. Simulated integrated difference counts $\int \mathcal{L} d\Sigma$ *vs.* $\phi_{\gamma\gamma}$ in a bin $2^\circ < \theta^{\rm lab}_{\gamma\gamma} < 3^\circ$ for integrated luminosity of 7200 / fb with Hall-A HRS-e $\otimes$0.01 sr photon calorimeter. The calorimeter is placed at $\theta_H = -11^\circ$ and $\theta_V = 2.5^\circ$ horizontal and vertical, respectively, relative to the beam. Similar yields are obtained simultaneously in bins $1^\circ < \theta^{\rm lab}_{\gamma\gamma} < 2^\circ$, $3^\circ < \theta^{\rm lab}_{\gamma\gamma} < 4^\circ$, & $4^\circ < \theta^{\rm lab}_{\gamma\gamma}$.